CrystEngComm

Accepted Manuscript

This is an *Accepted Manuscript*, which has been through the Royal Society of Chemistry peer review process and has been accepted for publication.

Accepted Manuscripts are published online shortly after acceptance, before technical editing, formatting and proof reading. Using this free service, authors can make their results available to the community, in citable form, before we publish the edited article. We will replace this *Accepted Manuscript* with the edited and formatted *Advance Article* as soon as it is available.

You can find more information about *Accepted Manuscripts* in the Information for Authors.

Please note that technical editing may introduce minor changes to the text and/or graphics, which may alter content. The journal's standard Terms & Conditions and the Ethical guidelines still apply. In no event shall the Royal Society of Chemistry be held responsible for any errors or omissions in this *Accepted Manuscript* or any consequences arising from the use of any information it contains.

ROYAL SOCIETY OF CHEMISTRY

www.rsc.org/crystengcomm

JournalName

RSC Publishing

ARTICLE

Synthesis and Aggregation Properties of A Series of Dumbbell Polyhedral-Oligosilsesquioxane-Perylene Diimide Triads

Cite this: DOI: 10.1039/x0xx00000x

Ying Zhang[a], Liangliang Zhang[b], Heyuan Liu[a], Di Sun[a], and Xiyou Li[a,*]

Received 00th January 2012,
Accepted 00th January 2012

DOI: 10.1039/x0xx00000x

www.rsc.org/

A series of perylenetetracarboxylic diimide (PDI) derivatives connected with two bulky polyhedral oligosilsequioxanes (POSS) were designed and synthesized for the purpose of revealing the effect of bulky and well-defined side groups on the self-aggregation behaviour of PDIs. The properties of these compounds in solution were investigated by UV-vis absorption spectra, fluorescence spectra, and fluorescence quantum yields. The results indicate that the POSS groups do not show large effects on the spectroscopy properties of PDIs in solution. However, the solid states spectroscopic properties of these compounds are significantly affected by the bulky POSS groups. The presence of bulky POSS groups changes the packing structure of the molecules in solid states and then affects the solid states emission properties. Our results revealed that the introduction of bulky POSS groups to the molecules will not inevitably lead to promoted solid state fluorescence quantum yield as expected. It is the packing structure of the molecules in solid state which determine the solid state fluorescence quantum yields. If the bulky POSS groups lead to the formation of "J" aggregates in solid states, then the solid state fluorescence quantum yields will be improved significantly. Otherwise, if the bulky POSS groups cause "H" type aggregation for the molecules, the solid state fluorescence quantum yields will be small.

Introduction

Perylenetetracarboxylic diimide (PDI) derivatives are a group of important organic dyes because of their various applications, such as organic field-effect transistors,[1-3] light emitting diodes, [4-11] and solar cells.[12,14] PDIs are well known for their excellent photochemical and thermal stabilities and high fluorescence quantum yields. But the varied applications of PDI in different fields require different photophysical or chemical properties, which can be achieved by introducing different substitutents at different positions of PDI molecules.

The substitution positions of PDI molecules can be divided into three categories, they are the imide N,N′ positions, the 1, 6, 7, 12 positions of the hydrocarbon core (the "bay" positions)[15] and the 2, 5, 8, 11 positions (the peripheral positions). The substituents at imide nitrogen atoms normally lead to significant improvement on solubility in conventional organic solvents. Normally, no significant change on the photophysical property can be observed with substitution at the imide position of PDIs due to nodes in both the HOMO and LUMO along the long axis.[16,17] However, the substitution at the bay positions can change the photophysical properties of PDI significantly by disturbing the plane conformation of PDI core or the frontier molecular orbital distribution on the molecule skeleton.[18,19] By changing the properties of the bay substituents, the absorption and fluorescence bands can be moved from visible region to near infrared region[20]. The peripheral substitution can improve the solubility of molecules in organic solvents and change the photophysical properties simultaneously without disturbing the planar configuration of PDI core. A recent report reveals efficient singlet fission in the crystal of a peripheral substituted PDI compound.[21] Among the numerous studies on the synthesis of new PDI compounds, reducing the exciton interactions by introducing different groups at different positions and thus increasing the fluorescence quantum yields at solid states became a very important part, because of the great application potential of these materials. Langhals and coworkers showed that the aggregation of PDI can be prevented by introducing steric inhibiting alkyl groups at the imide nitrogen atoms, and the resulted compound exhibits strong fluorescence in solid state.[22,23] Liu et al. successfully introduced β-cyclodextrin grafts into the imide N,N′ positions, this compound exhibit strong solid-state fluorescence and can probe the vapor of organic amines with high sensitivity.[24] Previous studies in our group have shown that the steric hindrance introduced by the substituents at bay positions affects the aggregation behavior of

CrystEngComm Accepted Manuscript

PDI molecules efficiently.[25] Water-soluble PDIs have been obtained by incorporating hydrophilic moieties, including polyglycerol dendrons[26] and Newkome dendrons,[27] to the imide N,N' positions, and PDI aggregation could be suppressed and fluorescence quantum yields could be improved in water.[26]

Polyhedral oligosilsequioxanes (POSS) molecules, with unique nanoscale cage-shaped structure, have been widely incorporated into polymers because of their excellent performances in tuning mechanical strength[28] and thermal stability,[29] and other physical characteristics.[28] Moreover, many POSS-based organic dyes, such as boron dipyrromethene (BODIPY),[30,31] porphyrin,[32] phthalocyanines,[33] and azobenzene compounds,[34] were prepared and showed some new superior properties, such as the reduced aggregation ability in solutions,[32] the improved photochemical stabilities[35] and so on. POSS-containing PDI was also prepared, and showed high sensitivity in rapid detection of fluoride ions in aqueous solution.[36] In the present work, we designed and synthesized a series of POSS-containing compounds with different substituents at the bay positions. The structures of these compounds are summarized in Scheme 1. This research was aimed at revealing the synergistic effect of substituents at the bay positions and POSS groups at the imide nitrogen atoms on reducing the aggregation of PDI molecules in solid states.

Experimental Section

Instrument and methods

^{1}H spectra were recorded on a Bruker 300 or 400 MHz NMR spectrometer with chemical shifts reported in ppm (TMS as internal standard). MALDI-TOF mass spectra were recorded with a Bruker/ultra flex instrument. Absorption spectra were measured on SHIMADZU UV-2450 spectrophotometer with a wavelength resolution of 0.3 nm. Steady state fluorescence spectra, and fluorescence lifetimes were measured on FLS920 (Edinburgh) fluorometer with excitation at 400 nm. Steady state fluorescence spectra were recorded by exciting the samples with Xe lamp. The wavelength resolution of the monochrometer is 0.1 nm. The fluorescence lifetime data were recorded following 445 nm excitation with a picosecond pulsed laser diode (EPL-445, Edinburgh Instruments). The fluorescence lifetimes were measured with a time correlated single photon counting (TSPC) methods. Solution fluorescence quantum yields were calculated with **1a** (100%, 5×10^{-6}M in chloroform) as standard. The absolute solid state fluorescence quantum yields were measured with integrating spheres on FLS920. Single-crystal X-ray diffraction data of **3b** and **3c** were collected with the use of Agilent Xcalibur Eos Gemini diffractometer with Enhance (Cu) X-ray Source (Cu-Kα, λ = 1.54178 Å). The data were collected at 150 K because the crystals lose solvent fast and have extensive disorder in the solvent sphere. Single-crystal X-ray diffraction data of **1b** was collected at room temperature. All absorption corrections were applied using the multiscan program SADABS. All structures were solved by direct methods using the SHELXS-97[37] program of the SHELXTL package and refined by the full-matrix least-squares method with SHELXL-97.[38]

The thin solid films of these compounds were prepared by dropping the solution of the compounds in chloroform to the cleaned surface of quartz (for the spectroscopy measurements and crystal silica (for XRD experiments). Single crystals suitable for X-ray diffraction were obtained by dissolving **1b** in $CHCl_3$, **3b** and **3c** in a mixture of $CHCl_3$/MeOH = 3:2, followed by slow evaporation of the solvents.

Materials

Aminopropylisobutyl POSS (AM0265) and p-aminophenylisobutyl POSS (AM0292) were purchased from Hybrid Plastics. Imidazole and o-dichlorobenzene (ODCB) were purchased from J&K. Perylene-3,4,9,10-tetracarboxylic dianhydride and other chemicals were purchased from commercial sources. Solvents were of analytical grade and used directly without any purification. **1a**[39] and **1c**[40] was prepared according to literatures. **1b**, **2a-c**, **3a-c** are synthesized by either method A or method B.

METHOD A: Perylene-3,4,9,10-tetracarboxylic dianhydride (0.05mmol)，amines (0.15 mmol) and imidazole (0.5g) in toluene (15ml) was heated to reflux under a nitrogen atmosphere and kept at reflux for 24h.[41] The solvent was removed under reduced pressure and the residue was washed with dilute hydrochloric acid (10%, 100 mL) and then water. The product was purified by column chromatography on silica gel (200 - 300 mesh). After recrystallization from chloroform and methanol, the product was collected and subjected to structure characterization.

METHOD B: Perylene-3,4,9,10-tetracarboxylic dianhydride (0.05mmol), p-aminophenylisobutyl POSS (0.15 mmol), imidazole (0.5 g), and 2 mL of o-dichlorobenzene (ODCB) were refluxed at 140 °C under nitrogen atmosphere for 6h. After cooling, the reaction mixture was dispersed in 20 mL ethanol and 20 mL HCl(2N). The mixture was extracted two times with 200 mL chloroform. The combined organic phase was washed with 5% $NaHCO_3$ aqueous solution until neutral, it was then concentrated, and purified by column chromatography on silica gel (200-300 mesh), after recrystallization from chloroform and methanol, the product was subjected to structure characterization.

1a: Method A. The product was purified by column chromatography with chloroform as eluent, and collected as a dark red solid with a yield of 90%. ^{1}H NMR ($CDCl_3$, 300 MHz, ppm): δ 8.67 (m, 8H), 4.22 (t, 4 H), 1.79 (m, 4 H), 1.29 (m, 20H), 0.89 (t, 6H). Anal. calcd for $C_{40}H_{42}N_2O_4$ (%): C 78.15, H 6.89, N 4.56; found: C 78.37, H 6.67, N 4.42.

1b: Method B. The product was purified by column chromatography with chloroform as eluent, **1b** was collected as red solid with a yield of 88%. ^{1}H NMR ($CDCl_3$, 300 MHz, ppm): δ 8.68 (m, 8H), 4.21 (m, 4H), 1.84 (m, 18H), 0.94 (m, 84H), 0.74 (t, 4H), 0.58 (m, 28H). MALDI-TOF (m/z): calcd 2102.64; found 2125.720 [M+Na$^+$]; Anal. calcd for $C_{86}H_{146}N_2O_{28}Si_{16}$ (%): C 48.99, H 7.12, N 1.28; found: C 49.06, H 6.99, N 1.33.

CrystEngComm Accepted Manuscript

This journal is © The Royal Society of Chemistry 2012

1c: Method B. Yield 43%. ^{1}H NMR ($CDCl_3$, 300 MHz, ppm): δ 8.76 (m, 8H), 7.87 (d, 4H), 7.37 (d, 4H), 1.91 (m, 14 H), 0.98 (m, 84H), 0.66 (m, 28H). Anal. calcd for $C_{92}H_{142}N_2O_{28}Si_{16}$ (%): C 50.84, H 6.59, N 1.29; found: C 50.59, H 6.74, N 1.21.

2a: Method A. The mixture was purified by column chromatography with dichloromethane/hexane (v/v = 5:4) as eluent, and **2a** was collected with a yield of 77%. ^{1}H NMR ($CDCl_3$, 300 MHz, ppm): δ 9.61 (d, 2H), 8.59 (d, 2H), 8.36 (s, 2H), 7.47 (t, 4H), 7.10 (t, 4H), 4.14 (t, 4 H), 1.75 (m, 4H), 1.37 (s, 18H), 1.25 (m, 20H), 0.86 (m, 6H). ^{13}C NMR ($CDCl_3$, 75 MHz, ppm): 162.2, 161.8, 154.4，151.5，147.2，132.3，129.0，128.1, 127.7，126.4，123.8，122.7，122.6,121.1, 118.1, 39.6, 33.5, 30.8, 30.4, 28.3, 28.2, 27.0, 26.1, 21.6, 13.1; MALDI-TOF (m/z): calcd 910.49; found 910.99 [M^+]. Anal. calcd for $C_{60}H_{66}N_2O_6$ (%): C 79.09, H 7.30, N 3.07; found: C 78.92, H 7.47, N 3.14.

2b: Method A. The mixture was purified by column chromatography with chloroform/hexane (v/v = 4:1) as eluent to give compound **2b** in yield of 45%. ^{1}H NMR ($CDCl_3$, 300 MHz, ppm): 9.63 (m, 2H), 8.60 (m, 2H), 8.37 (s, 2H), 7.45 (t, 4H), 7.10 (t, 4H), 4.14 (m, 4H), 1.82 (m, 18 H), 1.50 (s, 4H), 1.36 (s, 18H), 0.91 (m, 84H), 0.58 (m, 28H). ^{13}C NMR ($CDCl_3$, 75 MHz, ppm): 163.3, 162.9, 155.5, 152.7, 148.1, 133.5, 130.1, 129.4, 128.8, 127.4, 125.1, 123.9, 123.8, 122.3, 119.1, 42.9, 34.5, 31.5, 25.7, 23.84, 22.4, 21.5, 9.8; MALDI-TOF (m/z): calcd 2398.81; found 2400.15 [M+H$^+$]. Anal. calcd for $C_{106}H_{170}N_2O_{30}Si_{16}$ (%): C 53.01, H 7.13, N 1.17; found: C 52.87, H 7.24, N 1.07.

2c: Method B. The product was purified by column chromatography using hexane/dichloromethane (v/v= 3:2) as eluent. The product was collected with a yield of 61%. ^{1}H NMR ($CDCl_3$, 300 MHz, ppm): δ 9.64 (d, 2H), 8.60 (d, 2H), 8.40 (s, 2H), 7.82 (m, 4H), 7.46 (m, 4H), 7.32 (d, 4H), 7.12 (m, 4H), 1.50 (s, 4H), 1.36 (s, 18H), 0.91 (m, 84H), 0.58 (m, 28H). ^{13}C NMR ($CDCl_3$, 75 MHz, ppm): 163.7, 163.4, 156.1, 152.7, 148.7, 137.0, 135.4, 134.2, 133.2, 130.8, 129.9, 129.3, 128.0, 127.8, 125.6, 124.3, 124.1, 122.6, 119.6, 34.6, 31.5, 29.7, 25.7, 23.9, 22.6; MALDI-TOF (m/z): calcd 2466.78; found 2467.39 [M+H$^+$]. Anal. calcd for $C_{112}H_{166}N_2O_{30}Si_{16}$ (%): C 54.46, H 6.77, N 1.13; found: C 54.03, H 6.59, N 1.01.

3a: Method A. The mixture was purified by column chromatography with dichloromethane/hexane (v/v = 3:2) as eluent, and obtained as dark red solid in yield 56%. ^{1}H NMR ($CDCl_3$, 300 MHz, ppm): δ 8.22 (s, 4H), 7.22-7.25 (m, 8H), 6.80-6.84 (m, 8H), 4.08-4.12 (t, 4H), 1.62-1.69 (m, 4H), 1.23-1.29 (m, 56H), 0.83-0.86 (t, 6H). ^{13}C NMR ($CDCl_3$, 75 MHz, ppm): 163.3, 155.9, 152.9, 147.3, 132.9, 126.6, 122.5, 120.4, 119.9, 119.5, 119.3, 42.9, 34.4, 31.5, 25.69, 25.67, 23.8, 22.5, 22.4, 21.6, 9.75; MALDI-TOF (m/z): calcd 1206.67; found 1207.93 [M+H$^+$]. Anal. calcd for $C_{80}H_{90}N_2O_8$ (%): C 79.57, H 7.51, N 2.32; found: C 79.35, H 7.67, N 2.17.

3b: Method A. The resulting product was purified by column chromatography with dichloromethane/hexane (v/v = 3:2) as eluent, and collected as a red solid with a yield of 45%. ^{1}H NMR ($CDCl_3$, 300 MHz, ppm): δ 8.14 (s, 4H), 7.22 (m, 8H), 6.82 (m, 8H), 4.09 (t, 4H), 1.81 (m, 18H), 1.29 (s, 36H), 0.91(m, 84H), 0.56 (m, 32H); ^{13}C NMR ($CDCl_3$, 75 MHz, ppm): 162.4, 154.9, 151.9, 146.2, 131.9, 125.6, 121.5, 119.5, 118.8, 118.4, 118.3, 39.6, 33.3, 30.7, 30.4, 28.2, 26.1, 21.6, 13.0; MALDI-TOF (m/z): calcd 2694.99; found 2695.57 [M+H$^+$]. Anal. calcd for $C_{126}H_{194}N_2O_{32}Si_{16}$ (%): C 56.09, H 7.25, N 1.04; found: C 55.78, H 7.37, N 1.11.

3c: Method A. The desired product was further purified by column chromatography using hexane/dichloromethane (v/v = 3:2) as eluent to get compound **3c** in yield 48%. ^{1}H NMR ($CDCl_3$, 400 MHz, ppm): δ 8.27 (s, 4H), 7.79 (d, 4H), 7.25 (d, 12H), 6.87 (d, 8H), 1.88 (m, 14H), 1.29 (s, 36H), 0.95-0.99 (m, 84H), 0.64-0.66 (m, 28H). ^{13}C NMR ($CDCl_3$, 75 MHz, ppm): 163.7, 156.1, 152.8, 147.4, 137.0, 135.0, 133.2, 132.7, 127.7, 126.7, 122.6, 120.7, 120.2, 119.8, 119.4, 34.4, 31.41, 25.7, 23.9, 22.5. MALDI-TOF (m/z): calcd 2762.96; found 2762.70 [M^+]. Anal. calcd for $C_{132}H_{190}N_2O_{32}Si_{16}$ (%): C 57.31, H 6.92, N 1.01; found: C 56.56, H 7.03, N 0.92.

Results and discussion

Molecular design and synthesis

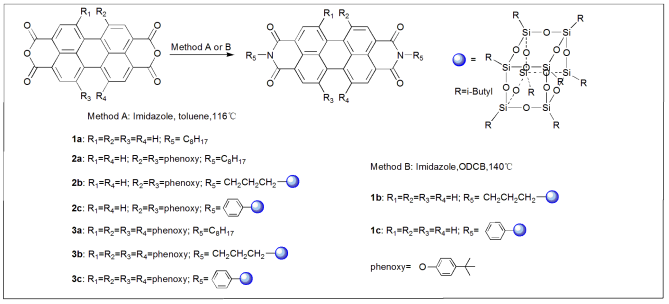

Scheme 1: Synthetic and molecular structures of compounds **1a-c**, **2a-c**, **3a-c**.

The effects of bulky substituents and branched alkyl tails on modifying phase structures and molecular packing have been nicely illustrated by previous studies.[42,43] Polyhedral oligosilsequioxanes (POSS), regarded as a small inorganic nanoparticle with diameter up to 1.5 nm,[44] were chosen as the bulky group because of their well-defined nature. The incorporation of POSS into organic molecules can bring remarkable improvement on the thermal and oxidative stability.[45] More importantly, the highly crystalline packing of POSS cages can sometimes aid the self-assembly in forming ordered structures in the solid state. Nevertheless, there are few reports on the systematic study of the effect of POSS on the self-assembly and ordered packing of π-conjugated materials[32] in the solid state. Therefore, POSS was chosen as a structural motif to couple with PDI as a model system to examine the effect of bulky groups at the imide nitrogen atoms and bay positions on the self-assemble of PDIs.

There are basically two ways to link POSS to both nitrogen atoms of PDI: through a rigid linkage or a flexible linkage. The former gives shape-persistent dumbbell-like molecules, while the latter gives relative flexible molecules. If

CrystEngComm Accepted Manuscript

the flexible linkage between POSS and PDI is used, the interaction between POSS and PDI will be small, and therefore, less influence is expected for the POSS on the self-assemble of PDIs.[46] Therefore, the POSS cages are covalently attached to PDI through both a flexible linkage and a rigid linkage.

The general synthetic procedures are shown in Scheme 1. All the new compounds were prepared by the coupling of 3,4,9,10-perylenetetracarboxylic dianhydried (PDA), 1,7-di(p-tert-butylphenoxy)perylene-3,4,9,10-tetracarboxylic dianhydride, and 1,6,7,12-tetra(p-tert-butylphenoxy)perylene-3,4,9,10-tetracarboxylic dianhydried with corresponding amino POSS. Two different methods are employed in the preparation of these compounds: method A (refluxing in imidazol/toluene) and method B (refluxing in imidazol/ODCB). Compounds **1a**, **2a-b**, and **3a-b** were prepared with method A and the rest of the compounds were prepared with method B. For the PDAs without substituents at the bay positions, the coupling between the dianhydried and amino-POSS was easier in imidazole/ODCB with higher production yields. Otherwise, for the PDA with bay position substitutions, the coupling will be easier in imidazole/toluene because of the improved solubility of PDAs. The molecular structure of these new compounds has been fully characterized by ^{1}H NMR, MALDI-TOF mass and elemental analysis.

Properties of these compounds in solution

The optical properties of these new compounds in solution were investigated by UV-Vis and fluorescence spectroscopy. The spectra of **2a-c**, **3a-c** are shown in ESI (Fig S1).

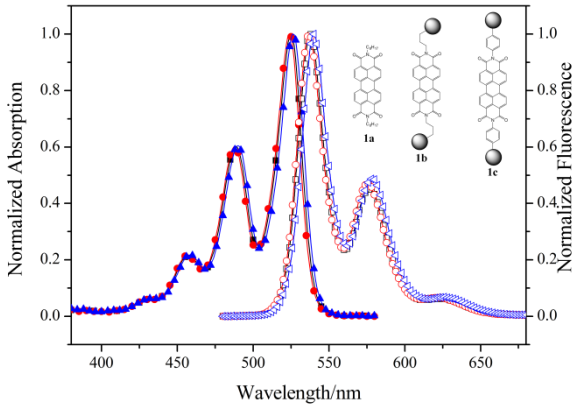

Fig. 1 UV-vis absorption (solid) and fluorescence spectra (hollow) of **1a** (black square), **1b** (red circle), **1c** (blue triangle) in chloroform (5.0×10^{-6}M) at room temperature. The inset shows the schematic molecular structure of **1a-c**.

Fig. 1 shows the absorption and emission spectra of **1a-c** in $CHCl_3$. All these three compounds (**1a-c**) exist as isolated molecules and non aggregate was found in the solution as revealed by the absorption spectra.[47] In the visible region, three pronounced absorption bands are observed respectively at 457 nm, 488 nm, 525 nm for **1a**. The band at 525 nm represents the lowest energy transition from the ground state to the first excited state, whilst the subsequent maxima at 488 and 457 nm correspond to transitions to the various excited vibrational levels of the first electronic excited state, consistent with the previous findings.[48,49,50] The absorption spectra of **1b** are identical to that of **1a**, no difference on the maximum absorption wavelength and molar extinction coefficient can be identified, which means the POSS groups linked by the flexible linkage at the imide nitrogen atoms do not interact with the PDI core. The absorption spectra of **1c** are also very similar with that of **1a** and **1b**, but a small red-shift (about 2 nm) on the absorption maximum can be identified. It is not a system error caused by instrument, because in one hand the wavelength resolution of the instrument (0.3 nm) is much smaller than the shift, on the other hand similar red-shifts have been found for **2c** and **3c** in comparison with their counterpart **2a** and **3a**, respectively. This means, even though the molecular orbital knots on the imide nitrogen atoms, the phenyl bridge has indeed influenced the absorption spectrum of PDI slightly.

By comparing the absorption spectra of **2a-c** and **3a-c** (Fig. S1(a,b) ESI) with those of **1a-c**, we can find that the introduction of phenoxyl groups at the bay position has caused significant red-shift on the maximum absorption peak, which can be attributed to the electron donating nature of the p-*tert*-butylphenoxy groups and can be explained by König's color theory.[51,52] It should also be noted that the cleanly resolved progressions of vibrational peaks observed in the absorption spectrum of **1a-c** is nearly lost in that of **2a-c** and **3a-c**. The band broadening observed can be attributed to two reasons. One could be the increase of the conjugation between the substituents and the perylene core.[53,54] Another could be the twisting of the PDI core by the substituent.[55,56]

The fluorescence emission spectra of compound **1a**, with a maximum at λ_{max} = 537 nm, is a mirror image of the S_0–S_1 absorption band. Identical fluorescence emission spectra with that of **1a** have been recorded for **1b**, indicating no interaction between POSS and PDI core in compound **1b**. Small red-shift can be identified for the fluorescence emission maximum of **1c** compared with that of **1a**, suggesting the weak interactions between the phenyl bridge and PDI core in compound **1c**, which is consistent with the results of absorption spectra. The Stokes shift of **1a** is 12 nm, which increased to 33 nm and 35 nm for **2a** and **3a,** respectively, owing to a pronounced vibronic progression and conformational disorder imparted by the core-twisted chromophores.[57]

Besides the absorption and emission spectra, the fluorescence quantum yields and fluorescence lifetimes are also measured for these compounds and the results are summarized in Table 1. The fluorescence intensity of all these compounds decays mono exponentially and only one fluorescence lifetime for each of them can be measured. The fluorescence lifetimes measured for **1a-c** are similar with each other, same results can be deduced from the fluorescence lifetimes of **2a-c** and **3a-c**, indicating no extra photoinduced process within these molecules has been introduced by POSS. Same result is suggested by the similar fluorescence quantum yields of them.

CrystEngComm Accepted Manuscript

This journal is © The Royal Society of Chemistry 2012

Table 1 . UV and fluorescence spectroscopic parameters of **1a-c**, **2a-c** and **3a-c** in $CHCl_3$ (5×10^{-6}M).

	λ_{abs} [a]/nm	ε[b]	λ_{em}/nm	τ(ns)	χ^2	Φ_f[c]
1a	525	9.3	537	4.28	1.00	1
1b	524	9.1	536	4.30	1.00	1
1c	526	9.5	539	4.01	1.00	0.92
2a	546	5.1	580	5.28	1.00	0.71
2b	545	4.9	579	5.22	1.00	0.71
2c	549	4.9	582	4.84	1.00	0.71
3a	583	5.1	618	6.76	1.01	0.46
3b	581	5.0	615	6.63	1.00	0.47
3c	586	5.2	620	6.19	1.00	0.44

[a] at the absorption maximum. [b] Molar absorption coefficient at the absorption maximum. ε: ($\times 10^4$ L.mol^{-1}.cm^{-1}). [c] With monomeric **1a** (5.0×10^{-6}M) as reference ($\Phi_f = 1$).

Aggregation of these compounds at solid state

The thin solid films of these compounds are prepared by casting a $CHCl_3$ solution of these compounds on the surface of substrate and then allow the solvents to evaporate gradually at room temperature. Because UV-vis absorption and fluorescence spectra are sensitive to the interchromophore distance and orientation,[58,59] and therefore, have been widely used to study the π-π stacking of organic dyes.[60,61,62] Moreover, a series of PDI dimers and oligomers with rigid molecular structure have been prepared and the absorption spectra have been reported, [41,59,63,64] which provides us good references to determine the packing structure of the PDI molecules in solid states by spectroscopy. So the packing structure of the molecules in solid state was first examined by the solid state absorption spectra. All the spectroscopic parameters of these compounds in solid states are summarized in Table 2 and the spectra are shown in Figure 2, 3 and 4.

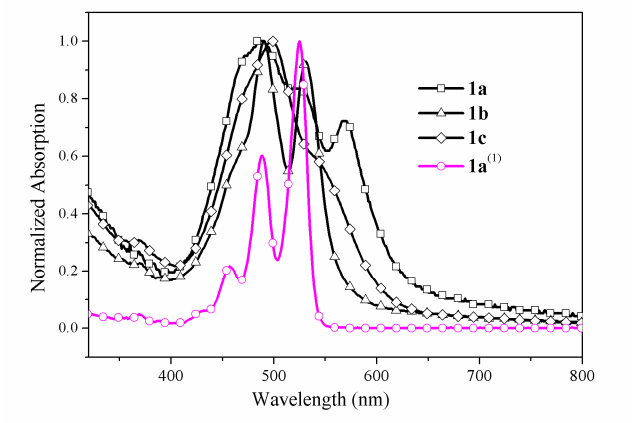

Fig. 2 Normalized absorption spectra of thin films of **1a-c**. (1): With monomeric **1a** (5.0×10^{-6}M in chloroform) as reference.

The absorption spectra of the thin solid films of **1a-c** are shown in Figure 2. The absorption spectra of **1a** in solution are also shown for the purpose of comparison. In the absorption spectra of **1a** thin solid film, several absorption bands appeared in the region of 400-600 nm, with the maximum absorption happened around 500 nm. Another small absorption band with a relatively smaller intensity can be found at 570 nm, which red shifted for about 46 nm in comparison with the 0-0 transition of **1a** in solution. The blue-shifting on the maximum absorption band can be attributed to the "H" type (face-to-face) interaction, [24, 65] while the red-shifted absorption band is a sign of the presence of "J" type aggregation (head-to-tail).[57,66] These spectral features of **1a** at solid state suggest that there are different relative orientations between the neighbour molecules of **1a**, which cause different changes on the absorption spectra. This is understandable, because there is no substituents at the bay positions and bulky groups at imide nitrogen atoms, the molecules of **1a** can approach each other from different directions and then cause different interactions between the molecules.

In the absorption spectra of **1b** thin solid films, Figure 2, two sharp absorption bands around 491 and 531 nm can be found. These two bands red-shifted slightly with respect to those of **1b** in solution with the one at 491 nm has the largest intensity. Because similar spectral changes (red shift and intensity reverse on the 0-0 and 0-1 vibration bands) have previously reported for a "face-to-face" stacked PDI dimer with longitudinal displacement,[63] we suggest that the molecules of **1b** in the solid films take similar relative orientations, i.e. stacking in a "face-to-face" way, but with longitudinal displacement between the neighbour PDI molecules. The absorption spectra of **1c** thin solid films show a broad absorption band with the maximum absorption at about 499 nm, which blue shifted for about 34 nm compared with the maximum absorption of **1a** in solution. This is a clear indication of the "face-to-face" stacked structure without large longitudinal displacement, i.e. "H" type aggregation.[41]

By comparing the absorption spectra of **1a**, **1b** and **1c** in solid states, we can conclude that there are different relative orientations between the molecules of **1a** in the solid sates, which brings different spectral changes against their spectra in solution. This may be ascribed to either the different microcrystallines in the solid states of **1a**, or different relative orientations between the neighbour molecules of **1a** along different directions in the solid state. However, after the POSS are connected by a flexible linkage, the interactions between the molecules of **1b** can be assigned to a slipped "face-to-face" structure with obvious longitudinal displacement. When POSS linked to the PDI core by rigid linkages, the molecules of **1c** in the solid states take "face-to-face" stacked structure too, but without significant longitudinal displacement.

The absorption spectra of **2a-c** in solid states are shown in Figure 3. The absorption spectra of **2a** in solid states present two broad and red-shifted absorption bands with respect to the spectra of it in solution, which indicates the formation of "face-to-face" stacked structure with large longitudinal displacement.[63] Based on the red-shift of the 0-0 and 0-1 transition absorption, we suggest that the molecules of **2a** in the solid state form "J" aggregates.[63] The absorption spectra of **2b** present also broad absorption bands, but the 0-1 vibration band has the largest intensity, this means the molecules of **2b** formed

CrystEngComm Accepted Manuscript

"H" aggregates in the solid states with small longitudinal displacement.[41] The absorption spectra of **2c** present two red-shifted absorption bands, with the 0-0 transition has the largest absorption intensity. This is a typical absorption pattern of "face-to-face" stacked aggregates with large longitudinal displacement, i.e. "J" type aggregates.[57,63,66]

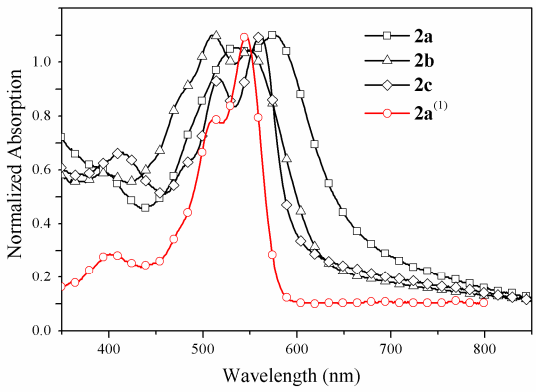

Fig. 3 Normalized absorption spectra of thin film of **2a-c**. (1): With monomeric **2a** (5.0×10^{-6}M in chloroform) as reference.

In general, as revealed by the absorption spectra of **2a-c** in solid states, **2a** and **2c** form "face-to-face" stacked structure with large longitudinal displacement in the solid states. Because the red-shift of the absorption band of **2c** is smaller than that of **2a**, the interaction between the molecules of **2c** in the solid states is weaker than that of **2a**, probably because of the steric hindrance caused by the bulky POSS groups, **2b** form "H" type aggregates in the solid states.

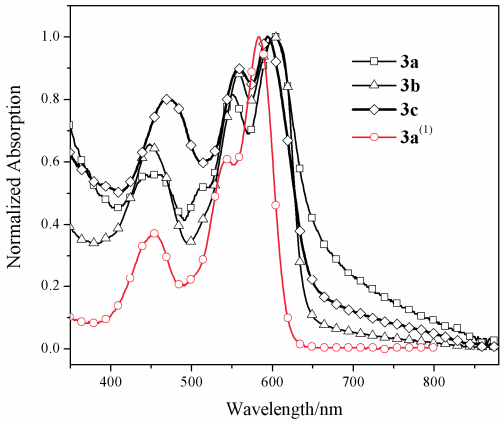

Fig. 4 Normalized absorption spectra of thin film of **3a-c**. (1) With monomeric **3a** (5.0×10^{-6}M in chloroform) as reference.

The solid state absorption spectra of **3a-c** are collected in Figure 4. PDIs with four phenoxyl groups have smaller tendency to from aggregates, because of the steric hindrance caused by the four bulky phenoxy groups at the bay positions.[25,41,57] In solution, they can only form "J" type aggregates with the help of hydrogen bonding or other strong supramolecular driving forces.[57] The solid state absorption spectra of **3a-c** do not show large difference from that of **3a** in solution except small red-shift on the maximum absorption wavelength. The maximum absorption band of **3a** and **3b** in solid state are similar. This means the introduction of POSS by flexible linkage does not bring large effects on the packing of the molecules in the solid states. The red-shift of the maximum absorption band of **3c** is smaller than that of **3b**, suggesting that the interactions between the molecules of **3c** in the solid states are smaller than that of **3b** and **3a**, this maybe ascribe to the rigid linkage between POSS and PDI, which makes the molecules of **3c** more shape-persistent and causes large steric hindrance between the neighbour molecules. Nevertheless, the red-shift on the absorption maximum suggests the formation of "J" type aggregates with slipped "face-to-face" stacked structure for these three compounds in solid states. Because of the steric hindrance caused by the bulky POSS at the imide nitrogen and phenoxyl groups at the bay positions, the interactions between the molecules of **3a-c** in solid states are small.[22,25]

Comparing the packing behaviours of **1a**, **2a** and **3a** in the solid states as revealed by the absorption spectra, we can conclude that without the bay substituents, the PDI molecules can approach a neighbour molecule from different directions and thus lead to different interactions between the molecules. When the bay substituents are introduced, the PDI molecules will prefer to interact with each other from the vertical direction of the PDI plane and form "face-to-face" stacked structure. The POSS groups linked at the end of the molecules have similar effects to that of the bay substituents as revealed by the compound series **1a-c**. But the effects of POSS groups on the packing structure of PDI molecules are complicated and changes in different molecules. We suggest that it is the result of synergetic effects of bay substituents and imide nitrogen substituents.

The packing structures of these molecules in solid state are also investigated by single crystal X-ray diffraction experiments. The single crystals are grown from chloroform, the same solvent for the thin solid film preparation, therefore, the crystal structure are good references for the structures of the thin solid films. Because crystals, which are suitable for single crystal X-ray diffraction experiments, have only been successfully grown for **1b**, **3b** and **3c**, only the crystal structures of these three compounds are measured (for details see ESI Table S1), crystallographic data for the three new crystal structures have been deposited with the Cambridge Crystallographic Data Center as supplementary publication no. CCDC 1022045, 1021968, and 1021969. And minute difference in the crystal structure of **1b** can be found comparing with the reported literature.[67] It is worth note that the quality of the crystals is poor for all these three compounds, due to the presence of freely rotating groups and solvent molecules. Therefore, the crystal data presented in the CIF files in the supporting information do no meet the usual standard. However,

CrystEngComm Accepted Manuscript

This journal is © The Royal Society of Chemistry 2012

the focus of this research is just a rough packing structure of the PDI cores, which is employed to confirm the results of UV-vis absorption spectra. So the poor crystal diffraction results are still meaningful for this research.

The crystal structure and molecular packing of **1b** have shown in Fig. 5 (a and b) and Fig. 6 (a and b). Molecules of **1b** crystallized in the triclinic space group *P-1*, POSS lie on the same direction, the conformation allowed more opportunity for the molecular packing. The two different views of **1b** reveal the π-scaffold is planar, the packing arrangement of PDI **1b** is a slipped "face-to-face" structure with longitudinal displacement, and the interplanar distance of two adjacent perylene skeleton planes are 3.61 Å (Fig. 6 b), which allows for slight π-π stacking, these are in agreement with absorption spectra.

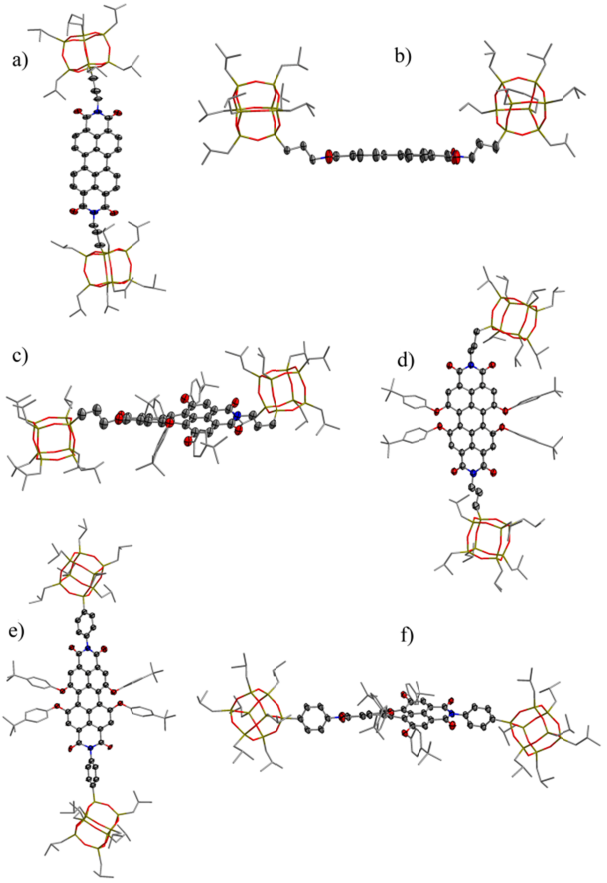

Fig. 5 Molecular structures of **1b** (a and b), **3b** (c and d), and **3c** (e and f) in front view (a, d and e) and side view (b, c, and f). Hydrogen atoms and all solvent molecules were omitted for clarity.

Fig. 5c and d show the molecular structure of **3b** as found in the crystal structure. **3b** crystallizes in the space group of P-1 with two co-crystallized $CHCl_3$ molecules. The cell contains 4 molecules (Z=2) in general positions (Fig. 6 (c and d)). The packing arrangement of PDI **3b** is characterized by two slipped stacks of strictly parallel chromophores. The interplanar distance of two adjacent perylene skeleton planes are 3.65 Å, which allows for slight π-π stacking. The two different views of **3b** reveal significant distortion of π-scaffold (Fig. 5(c, d)). We divide the perylene scaffold into two naphthalene subunits. The rotational twist of the averaged naphthalene planes with regard to each other is 27.5°, which was taken as the twist angle.[20] Indeed, the core twisting has significant effect on the molecular packing of **3b**.[68] The "J" type packing of the adjacent **3b** molecules can be seen clearly in Figure 6 (d). Besides this "J" type interaction, no other interactions should exist between the molecules of **3b** in the same unit cell or the molecules from other unit cells because of the large distance between them. This is in good agreement with the conclusion deduced from the absorption spectra.

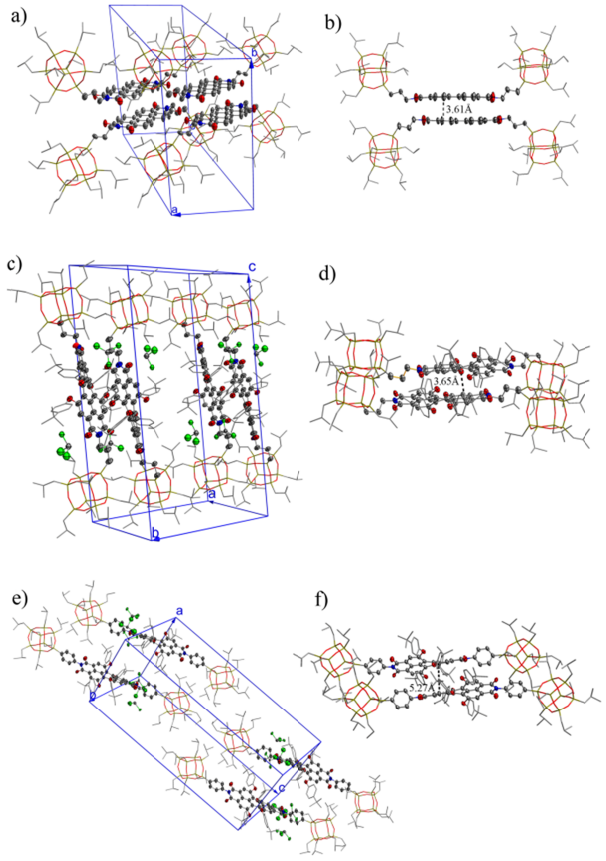

Fig. 6 Molecular packing of solvent-free **1b** (a and b), **3b** co-crystallized with 2 $CHCl_3$ (c and d), and **3c** co-crystallized with 3 $CHCl_3$ (e and f).

Fig. 5 (e and f) and Fig. 6 (e and f) show the molecular structures and molecular packing of **3c**. Single crystal X-ray diffraction analysis also shown that compound **3c** crystallizes in space group of P-1 with three co-crystallized $CHCl_3$ molecules. The cell contains 2 molecules (Z=2) in general positions. The two different views of **3c** (Fig. 5 e and f) reveal significant distortion of π-scaffold. The twist angle between the two naphthalene planes is 27.8(1)°, which is similar to **3b**. The

CrystEngComm Accepted Manuscript

packing arrangement of PDI **3c** in crystal is utterly slipped stack. Although PDI cores have slight π-π intermolecular interactions judged by the distance between the planes of PDI core, phenoxy groups have electronic interactions with the perylene diimide cores of adjacent molecules, these can have effect on the molecular packing. Similar to that found for **3b**, the interaction between the adjacent molecules in the crystal of **3c** is limited between two molecules. The interaction should be much weak because of the large distance between the two PDI core. The packing structure of **3c** in crystal corresponds also very well with that revealed by the absorption spectra. It must be noted that the consistency between the single crystal structure of **1b**, **3b** and **3c** with the predicated packing structure from their absorption spectra suggests that the predicated packing structure for other compounds (**1a, 1c, 2a-c** and **3a**) based on the absorption spectra should be also reliable.

We have also tried to determined the structure of the thin solid films by low angel X-ray diffraction experiments, but no one of the thin solid films can give any meaningful peaks in the diffraction patterns, which means the thin solid films prepared by casting chloroform solutions on the substrate do not have long range order (ESI Figure S3).

The solid state emission properties

As mentioned in the introduction part, the introduction of different groups at the imide nitrogen atoms of PDI, sometimes leads to strong solid emissions,[22] which is much favourable for photonics applications. The bulky POSS as well as the bay substituents can affect the packing structure of the PDI molecules in the solid films, therefore, they are expected to affect the fluorescence properties significantly too.

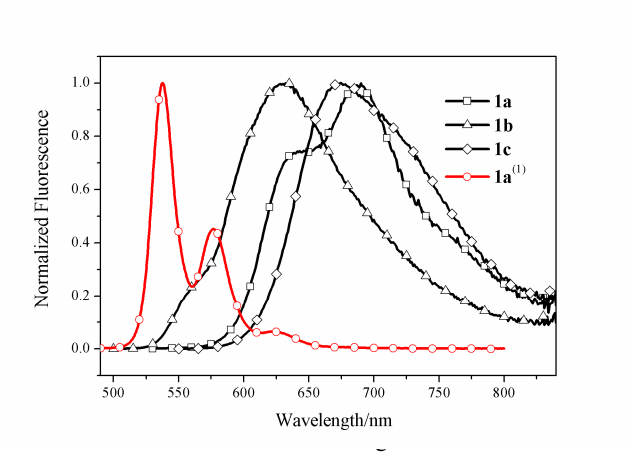

Fig. 7 The normalized fluorescence spectra of thin film **1a-c**. (1) With monomeric **1a** (5.0×10^{-6}M in chloroform) as reference.

The fluorescence properties of the solid films of these compounds are summarized in Table 2. Generally, the fluorescence maximums of the solid films red-shifted dramatically from that in solution, indicating the presence of strong excited state interactions between the neighbour molecules. Compound **3a-c** present relatively smaller red-shifts on the fluorescence maximum in these three series of compounds, which can be attributed to the reduced interactions among neighbour molecules due to the steric hindrance caused by the four phenoxyl groups attached at the bay positions.

Figure 7 compares the fluorescence spectra of **1a-c** with that of **1a** in solution. In the fluorescence spectrum of **1a**, two emission bands at about 630 and 700 nm can be identified. These fluorescence bands are roughly the mirror images of the absorption bands as shown in Figure 2 and can be attributed to the different absorptions in the absorption spectrum. The presence of multiple emission bands in the fluorescence spectrum suggests that the molecules of **1a** in the solid films do not pack uniformly, but with different structures, which is consistent with the results of the absorption spectrum. The broad low energy emission of **1a** can be assigned to the "excimer-like" sates.[69-71]

The maximum emission of **1b** happened at about 633 nm, which is significantly blue shifted compared with that of **1a** in solid sate, but red-shifted compared with that of **1a** in solution. This is a typical emission of a slipped "face-to-face" stacked PDI dimer with longitudinal displacement.[63] This suggests that the molecules of **1b** in solid state stacked in a "face-to-face" way, but with longitudinal displacement between the nearby molecules, which corresponds well with the absorption spectra of **1b** in Figure 1. The maximum emission wavelength of **1c** is about 680 nm, which is 50 nm longer than that of **1b**. Following the literatures,[69-71] this emission can be assigned to the "excimer-like" states.

Table 2 Absorption and fluorescence spectroscopic parameters of **1a-c**, **2a-c** and **3a-c** thin solid films.

	1a	**1b**	**1c**	**2a**	**2b**	**2c**	**3a**	**3b**	**3c**
λ_{abs} /nm	488	491	498	578	509	561	603	601	594
λ_{em} /nm	690	632	674	671	655	668	638	636	645
Φ_f* [%]	2.2	39.0	17.8	13.0	5.1	13.0	14.6	17.5	47.2

* Absolute fluorescence quantum yields measured by integrating spheres.

The absolute fluorescence quantum yields of these compounds are also measured and the results are summarized in Table 2. For compound series **1a-c**, **1a** presents the smallest solid sates fluorescence quantum, which is understandable because of the smallest groups attached and the molecules of **1a** can approach each other without steric hindrance. **1b** has the largest solid state fluorescence quantum yield among these three compounds, which is unexpected because the flexible linkage between the POSS groups and the PDI core would make the molecules of **1b** more flexible and then less steric hindrance when two **1b** molecules come close to each other. This will leave a short distance between the molecules of **1b** and principally a strong interaction between the PDI molecules. However, the shorter wavelength emission together with the

CrystEngComm Accepted Manuscript

This journal is © The Royal Society of Chemistry 2012

absorption character of **1b** suggest that it formed slipped "face-to-face" stacked structure with longitudinal displacement in solid state, while **1c** formed "H" type aggregates in the solid states without any indication of the presence of longitudinal displacement.[63] This is the reason why the solid state fluorescence quantum yield of **1b** is larger than that of **1c**.

The normalized fluorescence spectra of **2a-c** in solid states are shown in ESI Figure S2 (a). All these three compounds show similarly broad emission band in long wavelength region (660-680 nm), which can be assigned to the "excimer-like" states,[63] a typical feature of "face-to-face" stacked PDI molecules.[63,72] Due to the packing structures of these molecules in solid states are different from each other, the maximum emission wavelengths vary from 660 nm for **2b** to 680 nm for **2a** and **2c**. [41,63,72]

Among these three compounds, **2b** presents the smallest solid state fluorescence quantum yield, while the solid state fluorescence quantum yields of **2a** and **2c** are almost the same. Obviously, the bulky POSS group of **2b** and **2c** did not promote the solid state fluorescence quantum yields as expected. This can be attributed to the different packing structures of the molecules in solid states. **2a** and **2c** formed "J-type" aggregates as indicated by the red-shifted absorption bands,[63] while **2b** formed "H" aggregates as revealed by the blue shifted absorption maximum. This result tells again that the most important factor determining the solid state fluorescence quantum yields of **2a-c** is the packing structure of the molecules in solid state.

The solid state fluorescence spectra of **3a-c** are shown in ESI Figure S2 (b). The fluorescence spectra of these three compounds in solid state are similar with each other. The emission peaks of these three compounds shifted to longer wavelength compared with that of **3a** in solution, which can be attributed the interactions between the molecules. The absolute fluorescence quantum yields of **3a** and **3b** are similar to each other, which means that the POSS groups in **3b** do not benefit the solid states fluorescence quantum yield. However, the solid state fluorescence quantum yield of **3c** is significantly larger than that of **3a** and **3b**. As revealed by the red shift of the absorption bands with respect to that in solution and the crystal structure of these compounds, all these three compounds formed "J" type aggregates in solid states. But the red-shifts of **3a** and **3b** are almost identical, which means the interaction intensity between the neighbour molecules are the same. However, the red-shifts of the absorption bands of **3c** are significantly smaller than that of **3a** and **3b**, which means the intensity of the interactions between the neighbour molecules of **3c** is small, and thus the solid state fluorescence quantum yield of **3c** is larger than that of **3a** and **3b**.

By comparing the solid state fluorescence quantum yields of **1a**, **2a** and **3a**, we can conclude that the bay substituents can improve the solid state emission properties to some extent. However, the effects of bay substituents on promote the solid state fluorescence quantum yields in other two compound series (**1b, 2b, 3b** and **1c, 2c, 3c**) is not so significant. Compound **1b** and **3c** are the best two solid state emitters among these nine compounds. This result indicates that the introduction of bulky groups to a molecule will not inevitably lead to a significant improvement on the emission property. The crucial factor, which affects the solid state emission property, is the packing structure of the molecules in the solid state. Avoiding the formation of "H" type aggregates in solid states seems a rational strategy towards a good solid state emitter.

Conclusions

Three series of PDI compounds equipped with POSS groups via flexible or rigid linkage have been synthesized to clarify the synergistic effect of substituents at the bay positions and POSS groups at imide nitrogen on reducing the aggregation of PDI molecules in solid states. The POSS groups at the imide nitrogen bring large changes on the packing structure of the molecules in solid state. Based on the changes on the solid state absorption spectra against those in solution, the packing structure of the molecules in solid states are proposed and three of them have been verified by the crystal structure. Most of the molecules packed in a "face-to-face" way, but with different longitudinal displacement. Large longitudinal displacement leads to "J" type interactions between the neighbour molecules in solid states and large solid state fluorescence quantum yields, while the small longitudinal displacement causes "H" type interactions and small solid state fluorescence quantum yields. The packing structure of the molecules in solid states is the dominating factor to determine the solid state fluorescence quantum yields. The introduction of bulky groups in PDI molecules will not inevitably promote the solid state fluorescence quantum yields.

Acknowledgements

We thank the Natural Science Foundation of China (Grand No.21173136, and 91233108), the National Basic Research Program of China (973 Program: 012CB93280) and Shandong University for the financial support.

Notes and references

[a]Key Laboratory of Colloid and Interface Chemistry of Ministry of Education, Department of Chemistry, Shandong University, Shanda Nan Lu 27#, Jinan, Shandong, 250100, China. E-mail: xiyouli@sdu.edu.cn; Fax: +86-531-88564464.

[b]Department of Chemistry, College of Science (East china), China University of Petroleum, Qingdao, China, 266580.

§ Electronic Supplementary Information (ESI) available: [details of any supplementary information available should be included here]. See DOI: 10.1039/b000000x/

1 J. Mei, Y. Diao, A. L. Appleton, L. Fang and Z. Bao, *J. Am. Chem. Soc.*, 2013, **135**, 6724−6746.

2 C. R. Newman, C. D. Frisbie, D. A. da Silva, J. L. Bredas, P. C. Ewbank and K. R. Mann, *Chem. Mater.*, 2004, **16**, 4436–4451.

CrystEngComm Accepted Manuscript

3 B. A. Jones, M. J. Ahrens, M. H. Yoon, A. Facchetti, T. J. Marks and M. R. Wasielewski. *Angew. Chem. Int. Ed.*, 2004, **43**, 6363-6366.

4 P. Ranke, I. Bleyl, J. Simmerer, D. Haarer, A. Bacher and H. W. Schmidt, *Appl. Phys. Lett.*, 1997, **71**, 1332-1334.

5 M. A. Angadi, D. Gosztola and M. R. Wasielewski, *Mater. Sci. Eng. B*, 1999, **63**, 191–194.

6 S. Alibert-Fouet, S. Dardel, H. Bock, M. Oukachmih, S. Archambeau, I. Seguy, P. Jolinat and P. Destruel, *ChemPhysChem.*, 2003, **4**, 983–985.

7 P. Schouwink, A. H. Schäfer, C. Seidel and H. Fuchs, *Thin Solid Films*., 2000, **372**, 163-168.

8 T. Zukawa, S. Naka, H. Okada and H. Onnagawa, *J. Appl. Phys.* 2002, 91, 1171-1174.

9 J.-S. Heo, N.-H. Park, J.-H. Ryu and K.-D. Suh, *Adv. Mater.*, 2005, **17**, 822-826.

10 C. Ego, D. Marsitzky, S. Becker, J. Zhang, A. C. Grimsdale, K. Müllen, J. D. MacKenzie, C. Silva and R. H. Friend, *J. Am. Chem. Soc.*, 2003, **125**, 437-443.

11 Y. Tani , T. Seki , X. Lin , H. Kurata , S. Yagai and K. Nakayama, *Mol. Cryst. Liq. Cryst.*, 2013, **578**, 88–94.

12 J. Hua, F. Meng, F. Ding, F. Li and H. Tian, *J. Mater. Chem.*, 2004, **14**, 1849-1853.

13 F. G. Brunetti, R. Kumar and F. Wudl, *J. Mater. Chem.*, 2010, **20**, 2934-2948.

14 B. A. Gregg, *J. Phys. Chem. B.*, 2003, **107**, 4688-4698.

15 C. Huang, S. Barlow and S. R. Marder. *J. Org. Chem.*, 2011, **76**, 2386–2407.

16 M. J. Ahrens, M. J. Tauber and M. R. Wasielewski, *J. Org. Chem.*, 2006, **71**, 2107-2114;

17 J. Vura-Weis, M. A. Ratner and M. R. Wasielewski, *J. Am. Chem. Soc.*, 2010, **132**, 1738–1739.

18 C. Zhao, Y. Zhang, R. Li, X. Li and J. Jiang, *J. Org. Chem.*, 2007, **72**, 2402-2410.

19 C. -C. Chao and M. -k. Leung, Y. O. Su, K.-Y. Chiu, T. –H. Lin, S. –J. Shieh and S. –C. Lin, *J. Org. Chem.*, 2005, **70**, 4323-4331.

20 A. J. Jimenez, M.-J. Lin, C. Burschka, J. Becker, V. Settels, B. Engels and F. Würthner, *Chem. Sci.*, 2014, **5**, 608-619.

21 S. W. Eaton, L. E. Shoer , S. D. Karlen, S. M. Dyar, E. A. Margulies, B. S. Veldkamp, C. Ramanan, D. A. Hartzler, S. Savikhin, T. J. Marks and M. R. Wasielewski, *J. Am. Chem. Soc.*, 2013, **135**, 14701-14712.

22 H. Langhals, O. Krotz, K. Polborn and P. Myer, *Angew. Chem. Int. Ed.,* 2005, **44**, 2427-2428.

23 H. Langhals, R. Ismael and O. Yürük, *Tetrahedron.*, 2000, **56**, 5435–5441.

24 Y. Liu, K.-R. Wang, D.-S. Guo and B.-P. Jiang, *Adv. Funct. Mater.*, 2009, **19**, 2230-2235.

25 J. Feng, B. Liang, D.Wang, H. Wu, L. Xue and X. Li, *Langmuir* 2008, **24**, 11209-11215.

26 T. Heek, C. Fasting, C. Rest, X. Zhang, F. Würthner and R. Haag, *Chem. Commun.*, 2010, **46**, 1884–1886.

27 C. D. Schmidt, C. Böttcher and A. Hirsch, *Eur. J. Org. Chem.*, 2007, **33**, 5497–5505

28 M. Tanahashi, *Materials*, 2010, **3**, 1593–1619.

29 J. D. Lichtenhan, Y. A. Otonari, M. J. Carr, *Macromolecules*, 1995, **28**, 8435-8437.

30 L. Marta, P.-S. Mercedes, A.-G. Francisco and S. Roberto. *J. Mater. Chem.*, 2011, **21**, 12803–12811.

31 B. Trastoy, M. E. Pérez-Ojeda, R. Sastre and J. L.Chiara. *Chem. Eur. J.*, 2010, **16**, 3833–3841

32 J. Sun, Y. Chen, L. Zhao, Y. Chen, D. Qi, K. –M. Choi, D. –S. Shin, and J. Jiang, *Chem. Eur. J.*, 213, **19**, 12613–12618.

33 T. Ceyhan, A. Altindal, A. R. Özkaya, B. Salihd and Ö. Bekaroğlu, *Dalton Trans.*, 2009, 10318–10329.

34 J. Zhou, Y. C. Zhao, K. Yu, X. Zhou and X. Xie, *New J. Chem.*, 2011, **35**, 2781–2792.

35 P. A. Ledin, I. M. Tkachenko, W. Xu, I. Choi, V. V. Shevchenko, and V. V. Tsukruk, *Langmuir.*, 2014, **30**, 8856−8865.

36 F. Du, Y. Bao, B. Liu, J. Tian, Q. Li and R. Bai, *Chem. Commun.*, 2013, **49**, 4631—4633

37 G. M. Sheldrick, SHELXS-97, Program for X-ray Crystal Structure Determination, University of Göttingen, Germany, 1997.

38 G. M. Sheldrick, SHELXL-97, Program for X-ray Crystal Structure Refinement, University of Göttingen, Germany, 1997.

CrystEngComm Accepted Manuscript

 This journal is © The Royal Society of Chemistry 2012

39 C. Suspene and J. -P. Simonato, US Pat. Appl., US 2012/0116084 A1, 2010.

40 X. K. Ren, B. Sun, C. C. Tsai, Y. F. Tu, S. W. Leng, K. X. Li, Z. Kang, R. M. Van Horn, X. P. Li, M. F. Zhu, C. Wesdemiotis, W. B. Zhang and S. Z. D. Cheng, *J. Phys. Chem. B*, 2010, **114**, 4802–4810.

41 J. Feng, Y. Zhang, C. Zhao, R. Li, W. Xu, X. Li and J. Jiang, *Chem. Eur. J.*, 2008, **14**, 7000–7010.

42 S. W. Leng, B. Wex, L. H. Chan, M. J. Graham, S. Jin, A. J. Jing, K. U. Jeong, R. M. Van Horn, B. Sun, M. F. Zhu, B. R. Kaafarani and S. Z. D. Cheng, *J. Phys. Chem. B*, 2009, **113**, 5403–5411.

43 S. W. Leng, L. H. Chan, J. Jing, J. Hu, R. M. Moustafa, R. M. Van Horn, M. J. Graham, B. Sun, M. F. Zhu, K. U. Jeong, B. R. Kaafarani, W. B. Zhang, F. W. Harris and S. Z. D. Cheng, *Soft Matter.*, 2010, **6**, 100–112.

44 G. Z. Li, L. C. Wang, H. L. Ni and C. U. J. Pittman, *Inorg. Org. Polym.,* 2001, **11**, 123–154.

45 S. Xiao, M. Nguyen, X. Gong, Y. Cao, H. B. Wu, D. Moses and A. J. Heeger, *Adv. Funct. Mater.*, 2003, **13**, 25–29.

46 L. Cui, J. P. Collet, G. Q. Xu and L. Zhu, *Chem. Mater.*, 2006, **18**, 3503–3512.

47 F. Würthner, Z. J. Chen, V. Dehm and V. Stepanenko, *Chem. Commun.*, 2006, 1188–1190.

48 L. Zhao, T Ma, H. Bai, G. Lu, C. Li and G. Q. Shi, *Langmuir*, 2008**, 24***,* 4380-4387.

49 V. J. Sapagovas, V. Gaidelis, V. Kovalevskij and A. Undzenas, *Dyes and Pigments.*, 2006, **71**, 178-187.

50 H. Langhals, S. Demmig and H. Huber, *Spectrochim Acta*, 1988; **44A**: 1189.

51 H. Langhals, *Helv. Chim.*, 2005, **88**, 1309.

52 E. M. Calzado, J. M. Villalvilla, P. G. Boj, J. A. Quintana, R. Gómez, J. L. Segura and M. A. Díaz-García, *J. Phys. Chem. C.*, 2007, **111**, 13595-13605;

53 K. Sugiyasu, N. Fujita and S. Shinkai, *Angew. Chem. Int. Ed.*, 2004, **43**, 1229-1233.

54 C. Kohl, T. Weil, J. Qu and K. Müllen, *Chem. Eur. J.*, 2004, **10**, 5297-5310.

55 P. Osswald, D. Leusser, D. Stalke and F. Würthner, *Angew. Chem. Int. Ed.*, 2005, **44**, 250-253.

56 Z. Chen, M. G. Debije, T. Debaerdemaeker, P. Osswald and F. Würthner, *ChemPhysChem.*, 2004, **5**, 137-140.

57 E. K. Theo, W. Hao, S. Vladimir and F. Würthner. *Angew. Chem. Int. Ed.*, 2007, **46**, 5541 –5544.

58 P. M. Kazmaier and R. Hoffmann, *J. Am. Chem. Soc.*, 1994, **116**, 9684-9691.

59 J. M. Giaimo, J. V. Lockard, L. E. Sinks, A. M. Scott, T. M. Wilson and M. R. Wasielewski, *J. Phys. Chem. A.*, 2008, **112**, 2322-2330

60 W. Wang, L.-S. Li, G. Helms, H. –H. Zhou and A. D. Q. Li, *J. Am. Chem. Soc.*, 2003, **125**, 1120-1121.

61 K. Balakrishnan, A. Datar, R. Oitker, H. Chen, J. Zuo, L. Zang, *J. Am. Chem. Soc.*, 2005, **127**, 10496-10497.

62 K. Balakrishnan, A. Datar, T. Naddo, J. Huang, R. Oitker, M. Yen, J. Zhao, and L. Zang, J. Am. Chem. Soc., 2006, 128. 7390 – 7398

63 H. Liu, L. Shen, Z. Cao and X. Li, *Phys. Chem. Chem. Phys.*, 2014, **16**, 16399-16406.

64 J. M. Giaimo, A. V. Gusev and M. R. Wasielewski, *J. Am. Chem. Soc.*, 2002, **124**, 8530-8531.

65 Z. J. Chen, V. Stepanenko, V. Dehm, P. Prins, L. D. A. Siebbeles, J. Seibt, P. Marquetand, V. Engel and F. Würthner, *Chem. Eur. J.*, 2007, **13**, 436–449.

66 F. Würthner, Z. J. Chen, F. J. M. Hoeben, P. Osswald, C. C. You, P. Jonkheijm, J. von Herrikhuyzen, A. P. H. J. Schenning, P. P. A. M. van der Schoot, E. W. Meijer, E. H. A. Beckers, S. C. J. Meskers, and R. A. J. Janssen; *J. Am. Chem. Soc.*, 2004, **126**, 10611–10618.

67 D. Clarke, S. Mathewb, J. Matisons, G. Simon and B. W. Skelton, *Dyes and Pigments*., 2011, **92**, 659-667.

68 Z. J. Chen, U. Baumeister, C. Tschierske and F. Würthner, *Chem. Eur. J.*, 2007, **13**, 450 – 465.

69 J. M. McCrate and J. G. Ekerdt, *J. Phys. Chem. C.*, 2014, **118**, 2104−2114.

70 A. M. Ara, T. Iimori, T. Yoshizawa, T. Nakabayashi and N. Ohta, *Chem. Phys. Lett.*, 2006, **427**, 322–328.

71 K. E. Brown, W. A. Salamant, L. E. Shoer, R. M. Young, and M. R. Wasielewski, *J. Phys. Chem. Lett.*, 2014, **5**, 2588−2593.

CrystEngComm Accepted Manuscript

72 T. V. D. Boom, R. T. Hayes, Y. Y. Zhao, P. J. Bushard, E. A. Weiss and M. R. Wasielewski, *J. Am. Chem. Soc.*, 2002, **124**, 9582-9590

CrystEngComm Accepted Manuscript

This journal is © The Royal Society of Chemistry 2012